

# Do Ultraluminous X-Ray Sources Really Contain Intermediate-Mass Black Holes?

Kiki VIERDAYANTI and Shin MINESHIGE

*Yukawa Institute for Theoretical Physics, Kyoto University, Sakyo-ku, Kyoto 606-8502*

*kiki@yukawa.kyoto-u.ac.jp*

Ken EBISAWA

*Institute of Space and Astronautical Science, Japan Aerospace Exploration Agency (ISAS/JAXA),  
Yoshinodai 3-1-1, Sagami-hara, Kanagawa 229-8510*

and

Toshihiro KAWAGUCHI

*Department of Physics and Mathematics, Aoyama Gakuin University, Sagami-hara, Kanagawa 229-8558*

(Received 2006 July 21; accepted 2006 August 24)

## Abstract

An open question remains whether Ultraluminous X-ray Sources (ULXs) really contain intermediate-mass black holes (IMBHs). We carefully investigated the XMM-Newton EPIC spectra of four ULXs that were claimed to be strong candidates of IMBHs by several authors. We first tried fitting by the standard spectral model of disk blackbody (DBB) + power-law (PL), finding good fits to all of the data, in agreement with others. We, however, found that the PL component dominates the DBB component at  $\sim 0.3$  to 10 keV. Thus, the black hole parameters derived solely from the minor DBB component are questionable. Next, we tried to fit the same data by the “ $p$ -free disk model” without the PL component, assuming an effective temperature profile of  $T_{\text{eff}} \propto r^{-p}$ , where  $r$  is the disk radius. Interestingly, in spite of one less free-model parameter, we obtained similarly good fits with much higher innermost disk temperatures,  $1.8 < kT_{\text{in}} < 3.2$  keV. More importantly, we obtained  $p \sim 0.5$ , just the value predicted by the slim (super-critical) disk theory, rather than  $p = 0.75$  that is expected from the standard disk model. The estimated black hole masses from the  $p$ -free disk model are much smaller;  $M \lesssim 40 M_{\odot}$ . Furthermore, we applied a more sophisticated slim-disk model by Kawaguchi (2003, ApJ, 593, 69), and obtained good fits with roughly consistent black hole masses. We thus conclude that the central engines of these ULXs are super-critical accretion flows to stellar-mass black holes.

**Key words:** accretion, accretion disks — black hole physics — X-rays: individual (NGC 5204 X-1, NGC 4559 X-7, NGC 4559 X-10, NGC 1313 X-2) — X-rays: stars

## 1. Introduction

X-ray data analysis has become one of the most widely studied subjects, and has made great contributions to the progress of astrophysics. This is particularly true in the field of astrophysical black holes. Thanks to rapid improvements in the sensitivity of X-ray detectors, new types of X-ray sources have been discovered. Some of them seem to be black holes that were not known before.

Recent X-ray observations on many nearby spiral galaxies have shown that the X-ray radiation consists of emission from several discrete X-ray sources, such as hot gaseous media, active galactic nuclei (AGN), and those point-like off-center X-ray sources whose X-ray luminosities significantly exceed the Eddington luminosity of a neutron star (Fabbiano 1989). The bright point-like off-center X-ray sources that cannot be identified with young supernova remnants are known as ultraluminous X-ray sources (ULXs: e.g., Makishima et al. 2000; Ptak, Colbert 2004). The ULXs, despite the fact that they are very luminous ( $L_x \sim 10^{39-41}$  erg s $^{-1}$ ), cannot be explained as collections of many sources with each luminosity less than the Eddington limit, since many of the ULXs exhibit significant time variabilities (e.g., Makishima et al. 2000). Therefore, one reasonable assumption is that the ULXs are single compact

objects powered by accretion flow. Then, how can we understand the extremely large luminosities exceeding the Eddington luminosity for a mass of  $\sim 10 M_{\odot}$ ?

A possibility that ULXs are only bright toward our line of sights (beaming model) was proposed (e.g. King et al. 2001; Körding et al. 2002; Reynolds et al. 1997), but is not generally accepted now. In fact, Wang (2002) has shown the existence of a bright nebula surrounding the ULX M 81 X-9, and some ULXs also exhibit extended optical nebulae (Pakull, Mirioni 2002). There is evidence that some ULXs are associated with a spreading wave of star formation, which supports the idea that many ULXs, particularly those located in star-forming galaxies, are high-mass X-ray binaries (King 2004). These facts indicate that the ULX surrounding nebulae are powered by the central high-mass X-ray sources, and that strong X-ray beaming toward our direction is unlikely.

Then, the question is, how massive are the central compact objects. At present, there are basically two distinct lines of thought: sub-Eddington accretion onto an intermediate (several hundreds  $M_{\odot}$ ) mass black hole (IMBH) and super-Eddington (super-critical) accretion onto a stellar-mass black hole. The success in fitting several ULXs spectra with a multicolor disk blackbody (DBB) and a power-law (PL) model supports the idea of IMBHs for the ULXs (Miller et al. 2003, 2004; Cropper

et al. 2004; Roberts et al. 2005), since the cool inner disk temperatures and the large innermost radii, obtained through model fitting, suggest a black hole mass within the IMBH range. The other line of thought, supporting a super-Eddington accretion flow, is the slim-disk model with stellar-mass black holes (Watarai et al. 2001; Kawaguchi 2003; Ebisawa et al. 2003; Okajima et al. 2006). The present article concerns with the super-Eddington thick accretion disks introduced in the early 1980s by the Warsaw group and their collaborators (e.g. Abramowicz et al. 1978, 1980) and with slim accretion disks, introduced in the late 1980s by the Warsaw and the Kyoto groups (Abramowicz et al. 1988, 1989). In these papers, the very possibility of super-Eddington beaming in thick accretion disk funnels, crucial for arguments presented here, was explicitly recognized, discussed, and stressed.

The IMBH notion faces a serious problem that the formation of IMBH itself remains unsettled (e.g., Madhusudhan et al. 2006). In contrast, the alternative possibility of super-critical accretion has been poorly investigated so far, due mainly to our limited knowledge about the properties of super-critical flow. The situation has been remarkably improved during the past few years, however, since basic tools for investigating high-luminosity accreting systems are now available. In the present paper, we consider the XMM-Newton EPIC spectra of the four ULXs, which had been claimed to be strong IMBH candidates, using theoretical super-critical models to see whether super-critical accretion takes place in these ULXs or not. Our final goal is to determine the mass of the central black holes and settle the issue regarding the origin of ULXs.

We applied accretion-disk spectral models to the observed ULX energy spectra, constrained the inner-most disk radius, and estimated the black hole mass. A very similar method to that used in the present paper was successfully applied to galactic black hole binaries (e.g., Ebisawa et al. 1991, 1993; Gierliński et al. 2001). Several authors have recently made elaborate mass and angular momentum estimates by spectral fitting for microquasars, i.e. by a very similar method to the one used in the present work (Shafee et al. 2006; McClintock et al. 2006; Davis et al. 2006). In the present study, however, we focused on a mass estimation and did not attempt to estimate the spin of the black hole.

The mass of the ULXs can also be accurately estimated by a different method than that described in our article. For this other independent estimate, double-peak QPOs in the 3 : 2 resonance should be detected in ULXs (Abramowicz et al. 2004). This is because these QPOs scale inversely with the mass of the source, which was first shown for microquasars by McClintock and Remillard (2006), and more recently for low-mass Seyfert galaxies by Lachowicz et al. (2006). There is also an indication that the same scaling is true for a (possible) detection of double-peak 3 : 2 QPOs in Sgr A\* (Török 2005), while for the ULXs, in general, it has not yet been detected. According to Mucciarelli et al. (2006), the only ULX where a QPO has been discovered at present is M82 X-1. By scaling the frequency inversely to the BH mass, the observed QPO frequency range (from a few tens to a few hundreds mHz) would yield a black hole mass anywhere in the interval from a few ten to a few thousand solar masses (Strohmayer, Mushotzky 2003; Mucciarelli et al. 2006).

The plan of this paper is as follows. We first describe the X-ray data that we used in the present study and our fitting methods in section 2. In section 3, we give the results of fitting, together with their implications on the black hole mass and mass-accretion rates. Section 4 is devoted to a discussion, and the final section 5 concludes the paper.

## 2. Data and Fitting Methods

### 2.1. Data

We performed spectral analyses of four ULXs by using XMM-Newton observational data. The data were extracted using the XMM-Newton SAS version 6.5.0 tools. The detailed extraction process will be explained separately for each object. Response files were made using the SAS tools `rmfgen` and `arfgen` for all data.

#### 2.1.1. NGC 5204 X-1

NGC 5204 X-1 is located  $\sim 0.3$  kpc from the center of a nearby,  $D = 4.8$  Mpc, Magellanic-type galaxy (Roberts, Warwick 2000). The typical X-ray luminosity of this source is on the order of  $2\text{--}6 \times 10^{39}$  ergs $^{-1}$  (0.5–8 keV) (Roberts et al. 2005).

NGC 5204 X-1 data for our analysis were obtained on 2003 January 6 (observation ID 0142770101). Following Roberts et al. (2005), we set `flag = 0` and `pattern  $\leq$  4` for pn data, while `#XMMEA_EM flag` and `pattern  $\leq$  12` were used for the MOS data. No time filters were applied to the data, since the background was less than 10 counts $^{-1}$  in the pn detector. The source spectra and light curves were extracted in a 36'' radius circle centered on the source; a 44'' radius nearby region was used to produce background data.

#### 2.1.2. NGC 4559 X-7 and X-10

NGC 4559 X-7 and X-10 are two of the brightest sources in NGC 4559 ( $D = 9.69$  Mpc). X-7 was located in the outer spiral arms, while X-10 was about 0.3 kpc from the optical nucleus of NGC 4559. They are also known as X1 and X4 respectively in Roberts and Warwick (2000), and IXO 65 and IXO 66 in Colbert and Ptak (2002) respectively (Cropper et al. 2004).

Data were obtained on 2003 May 27 (observation ID 0152170501) for both X-7 and X-10. However, X-10 was only seen in EPIC-pn, since the EPIC-MOS cameras were operated in the small-window mode. Following Cropper et al. (2004), we used 30'' radius centered on the source for X-7, while for X-10 we used 20'' radius with an exclusion of 6'' radius centered on the nucleus of the galaxy (12<sup>h</sup>35<sup>m</sup>57<sup>s</sup>.64, +27°57'35".8, J2000.0). A source-free region on the same CCD was selected as background for the EPIC-pn data, while regions as close as possible to the source were selected for EPIC-MOS X-7 data. The MOS data were filtered using `pattern  $\leq$  12` and `#XMMEA_EM flag`, while the pn data were filtered using `pattern  $\leq$  4` and `#XMMEA_EP flag`.

#### 2.1.3. NGC 1313 X-2

NGC 1313 X-2 is one example of ULX sources in a nearby spiral galaxy, NGC 1313 ( $D = 3.7$  Mpc). This ULX is located at approximately 8 kpc from the photometric center of the galaxy (Colbert et al. 1995). The data for our analysis were obtained on 2000 October 17 (observation ID 0106860101).

We performed the standard procedures, but somehow failed to create response files for the MOS data, leaving us only

**Table 1.** Fitting results with DBB + PL and  $p$ -free models.\*

Parameter	NGC 5204 X-1	NGC 4559 X-7	NGC 4559 X-10	NGC 1313 X-2
<b>DBB + PL</b>				
$N_{\text{H}}$	$0.51 \pm 0.11$	$1.58 \pm 0.19$	$0.98 \pm 0.22$	$1.98 \pm 0.27$
$kT_{\text{in}}$	$0.25 \pm 0.03$	$0.17 \pm 0.09$	$0.48 \pm 0.25$	$0.27 \pm 0.04$
Norm.	$3.7 \pm 2.6$	$46.9 \pm 30.3$	$0.04 \pm 0.11$	$4.5 \pm 4.0$
$\Gamma$	$1.92 \pm 0.06$	$2.17 \pm 0.05$	$1.94 \pm 0.13$	$2.01 \pm 0.13$
Norm.	$(3.02 \pm 0.48) \times 10^{-4}$	$(2.10 \pm 0.24) \times 10^{-4}$	$(2.01 \pm 0.83) \times 10^{-4}$	$(2.02 \pm 0.73) \times 10^{-4}$
$f_{\text{x}}$	$1.66 \times 10^{-12}$	$8.36 \times 10^{-13}$	$9.42 \times 10^{-13}$	$8.63 \times 10^{-13}$
$\chi^2/\text{dof}$	1.05	0.96	0.93	0.98
<b><math>p</math>-free</b>				
$N_{\text{H}}$	$0.34 \pm 0.01$	$0.60 \pm 0.06$	$0.91 \pm 0.08$	$1.42 \pm 0.14$
$kT_{\text{in}}$	$2.54 \pm 0.34$	$1.84 \pm 0.16$	$3.16 \pm 0.71$	$2.03 \pm 0.35$
$p$	$0.50 \pm 0.03$	$0.50 \pm 0.03$	$0.51 \pm 0.06$	$0.50 \pm 0.05$
Norm.	$(5.04 \pm 6.11) \times 10^{-4}$	$(1.04 \pm 0.85) \times 10^{-3}$	$(1.51 \pm 3.13) \times 10^{-4}$	$(8.13 \pm 12.9) \times 10^{-4}$
$f_{\text{x}}$	$1.55 \times 10^{-12}$	$7.96 \times 10^{-13}$	$9.14 \times 10^{-13}$	$8.08 \times 10^{-13}$
$\chi^2/\text{dof}$	1.12	1.19	0.93	1.15

\*  $N_{\text{H}}$  is an absorption column external to our Galaxy in units of  $10^{21}$  atom  $\text{cm}^{-2}$ . A Galactic absorption column is assumed as in the text.  $kT_{\text{in}}$  is the inner disk temperature in keV. The normalization for DBB and  $p$ -free is defined by  $[(R_{\text{in}}/\text{km})/(D/10 \text{ kpc})]^2 \cos i$ , where  $R_{\text{in}}$  is the inner disk radius,  $D$  the distance to the source, and  $i$  the angle of the disk. The unit of power-law normalization is photons  $\text{s}^{-1} \text{cm}^{-2} \text{keV}^{-1}$  at 1 keV.  $f_{\text{x}}$  is the observed flux in units of  $\text{erg cm}^{-2} \text{s}^{-1}$  (0.3–10 keV) that depends on the model.

the pn data to be analyzed. We set  $\text{flag} = 0$  and  $\text{pattern} \leq 4$  for the pn-data. Following Miller et al. (2003), we used  $24''$  radius centered on the source to obtain source spectra, while background counts were extracted in an annulus between  $24''$  and  $30''$ .

## 2.2. Fitting Methods

The source spectra were grouped to a minimum of 20 count  $\text{bin}^{-1}$  before fitting using XSPEC version 11.3. We first tried the standard spectral model of disk blackbody (DBB) + power-law (PL). We used the results as comparisons with other papers. Next, we tried to fit the data by the “ $p$ -free disk model”, assuming the effective temperature profile of  $T_{\text{eff}} \propto r^{-p}$ , where  $r$  is the disk radius (Mineshige et al. 1994). The  $p$ -free model is a potentially useful spectral model, since despite its simpleness it is very powerful for discriminating a slim disk with  $p \sim 0.5$  from the standard disk with  $p = 0.75$  (Watarai et al. 2000).

We also tried to fit the data with a more sophisticated slim-disk model calculated by Kawaguchi (2003), who calculated more realistic emergent spectra of super-critical flow based on the slim-disk model, taking into account relativistic and Compton-scattering effects. We will show the results separately apart from those two mentioned above, to avoid muddle, and we will give a brief comment on these results.

The effect of Galactic absorption was taken into account by using the wabs model (in XSPEC), where we fixed the value at  $1.5 \times 10^{20} \text{ cm}^{-2}$  for NGC 5204 X-1 and NGC 4559 X-7 and X-10, and  $3.9 \times 10^{20} \text{ cm}^{-2}$  for NGC 1313 X-2 from Dickey and Lockman (1990). The effect of absorption external to our Galaxy was also considered, and again we used the wabs model, but we let this value free throughout the fitting.

## 3. Spectral Analysis

The results of spectral analysis for each ULX investigated in the present work will be presented separately for three distinct spectral models: DBB + PL models (in subsections 3.1 and 3.2),  $p$ -free models (in subsection 3.3), and Kawaguchi’s models (in subsection 3.4). In addition, we summarize the fitting results in table 1.

### 3.1. DBB + PL Model

We first present our results of fitting based on the conventional approach; i.e., by using the DBB + PL model. As will be explicitly demonstrated below, we will basically confirm the previous results supporting the IMBH hypothesis.

#### 3.1.1. NGC 5204 X-1

We fit the MOS data over 0.3–8 keV and the pn data over 0.3–10 keV. We obtained a good fit to the data with the DBB + PL model (see figure 1). The reduced chi-squared is 1.05 with an inner-disk temperature of  $kT_{\text{in}} = 0.25 \pm 0.03 \text{ keV}$ , and a photon index of  $\Gamma = 1.92 \pm 0.06$ . The low temperature obtained from the fitting apparently supports the IMBH interpretation of ULXs, in agreement with Roberts et al. (2005). The flux obtained from the fitting by using this model is  $f_{\text{x}}(0.3\text{--}10 \text{ keV}) = 1.66 \times 10^{-12} \text{ erg cm}^{-2} \text{ s}^{-1}$ . These are in reasonable agreement with the previous results by Roberts et al. (2005); that is,  $kT_{\text{in}} = 0.21 \pm 0.03 \text{ keV}$  and  $\Gamma = 1.97 \pm 0.07$ .

#### 3.1.2. NGC 4559 X-7 and X-10

We next fit both the MOS and the pn data for NGC 4559 X-7 and the pn data for NGC 4559 X-10 over 0.3–10 keV. As before, we fit the data with the DBB + PL model and we obtained reduced chi-square values of 0.96 and 0.92 for X-7 and X-10, respectively. The inner-disk temperature,  $kT_{\text{in}} = 0.17 \pm 0.09 \text{ keV}$  and  $\Gamma = 2.17 \pm 0.05$ , were obtained for NGC 4559 X-7, while  $kT_{\text{in}} = 0.48 \pm 0.25 \text{ keV}$  and  $\Gamma = 1.94 \pm 0.13$  were

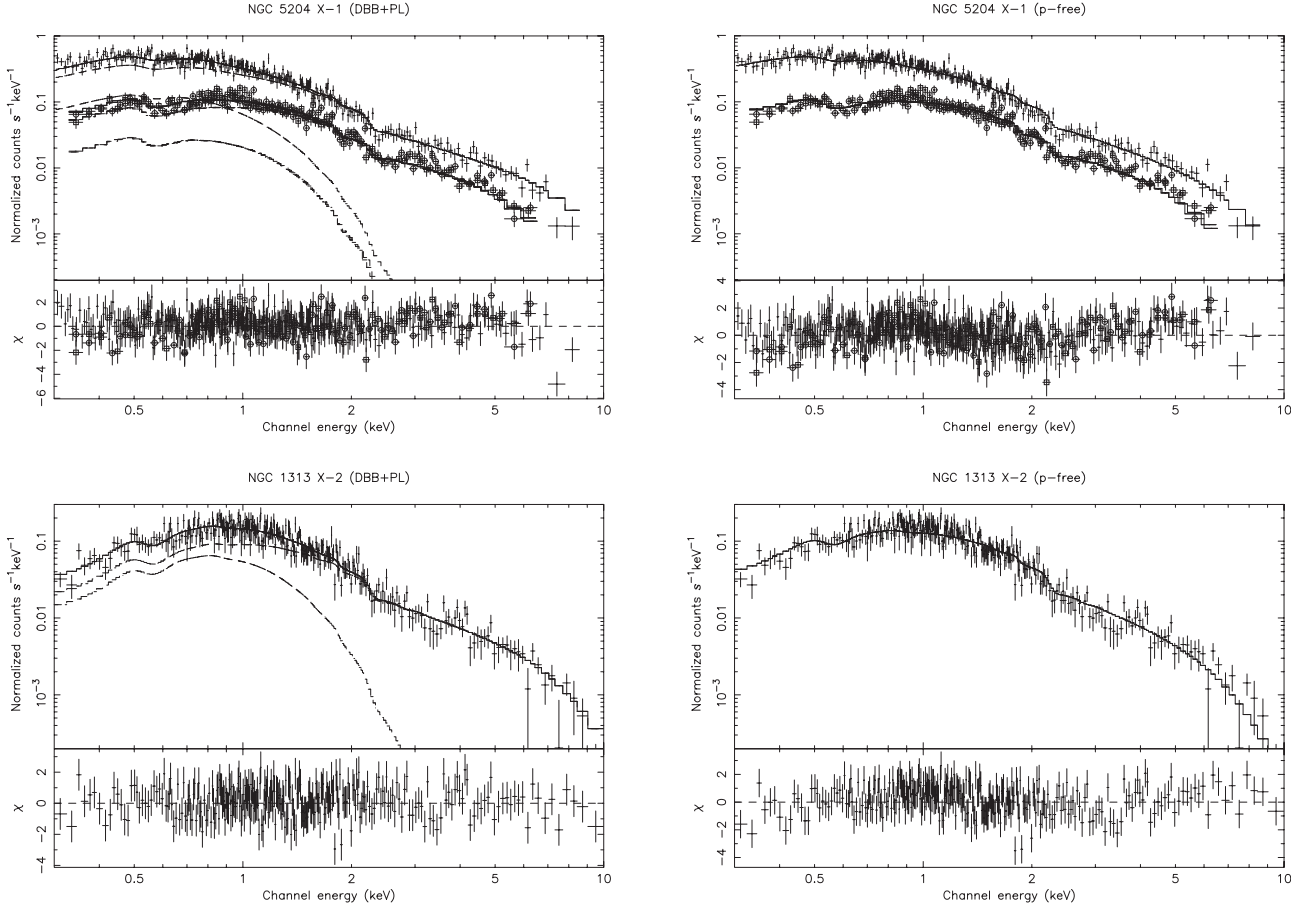


**Fig. 1.** Best-fit spectra and the fit residuals with the DBB + PL model (left panels) and  $p$ -free disk model (right panels) for NGC 5204 X-1, NGC 1313 X-2, NGC 4559 X-7 and X-10. The open circles, open squares, and dots represent mos1, mos2, and pn data, respectively. The dashed lines in the left panels represent the spectral components.

obtained for NGC 4559 X-10. However, for the case of X-10, we could actually obtain a good fit by the PL model alone, giving reduced chi-square values of 0.92 and  $\Gamma = 1.99 \pm 0.03$ .

For reference, the previous fits by Cropper (2004) obtained  $kT_{\text{in}} = 0.148 \pm 0.006$  keV, and  $\Gamma = 2.23 \pm 0.05$  for X-7, in good agreement with our results. As for X-10, Cropper et al. (2004) only showed the fitting result with the single component power-law.

### 3.1.3. NGC 1313 X-2

We fit the pn data of NGC 1313 X-2 over 0.2–10 keV with the DBB + PL model and found a good fit with a reduced chi-square value of 0.96. As in previous cases, we obtained a low inner-disk temperature,  $kT_{\text{in}} = 0.27 \pm 0.04$  keV and  $\Gamma = 2.01 \pm 0.13$ .

For a comparison, Miller et al. (2003) found  $kT_{\text{in}} = 0.16 \pm 0.16$  keV and  $\Gamma = 2.3 \pm 0.2$ , for NGC 1313 X-2, from fitting the MOS data with the DBB + PL model. The difference in the detectors is likely to be the origin of the small discrepancies.

## 3.2. Interpretation Based on DBB + PL Model

### 3.2.1. Basic methodology to derive black-hole mass

When we obtain a good fit to the observed spectra by the DBB model, we can easily estimate the black-hole mass and the Eddington ratio,  $L/L_E$  (with  $L$  and  $L_E$  being disk

luminosity and the Eddington luminosity, respectively), based on the standard disk theory. The basic methodology is summarized in Makishima et al. (2000).

Following Makishima et al. (2000), the bolometric luminosity of an optically thick accretion disk can be written as

$$L_{\text{bol}} = 2\pi D^2 f_{\text{bol}} (\cos i)^{-1} \quad (1)$$

with  $i$  being the inclination of the disk ( $i = 0$  corresponds to face-on geometry) and  $D$  the distance. This  $L_{\text{bol}}$  is related to the maximum disk color temperature,  $T_{\text{in}}$ , and the innermost disk radius,  $R_{\text{in}}$ , as

$$L_{\text{bol}} = 4\pi (R_{\text{in}}/\xi)^2 \sigma (T_{\text{in}}/\kappa)^4, \quad (2)$$

where  $\kappa \sim 1.7$  (Shimura, Takahara 1995) is the ratio of the color temperature to the effective temperature, or the spectral hardening factor, and  $\xi = 0.412$  is a correction factor reflecting the fact that  $T_{\text{in}}$  occurs at somewhat larger values than  $R_{\text{in}}$ . Hence, the innermost disk radius is

$$R_{\text{in}} = \xi \kappa^2 \sqrt{\frac{L_{\text{bol}}}{4\pi \sigma T_{\text{in}}^4}}. \quad (3)$$

We may identify  $R_{\text{in}}$  with the radius of the last stable Keplerian orbit. Thus, we may in general write

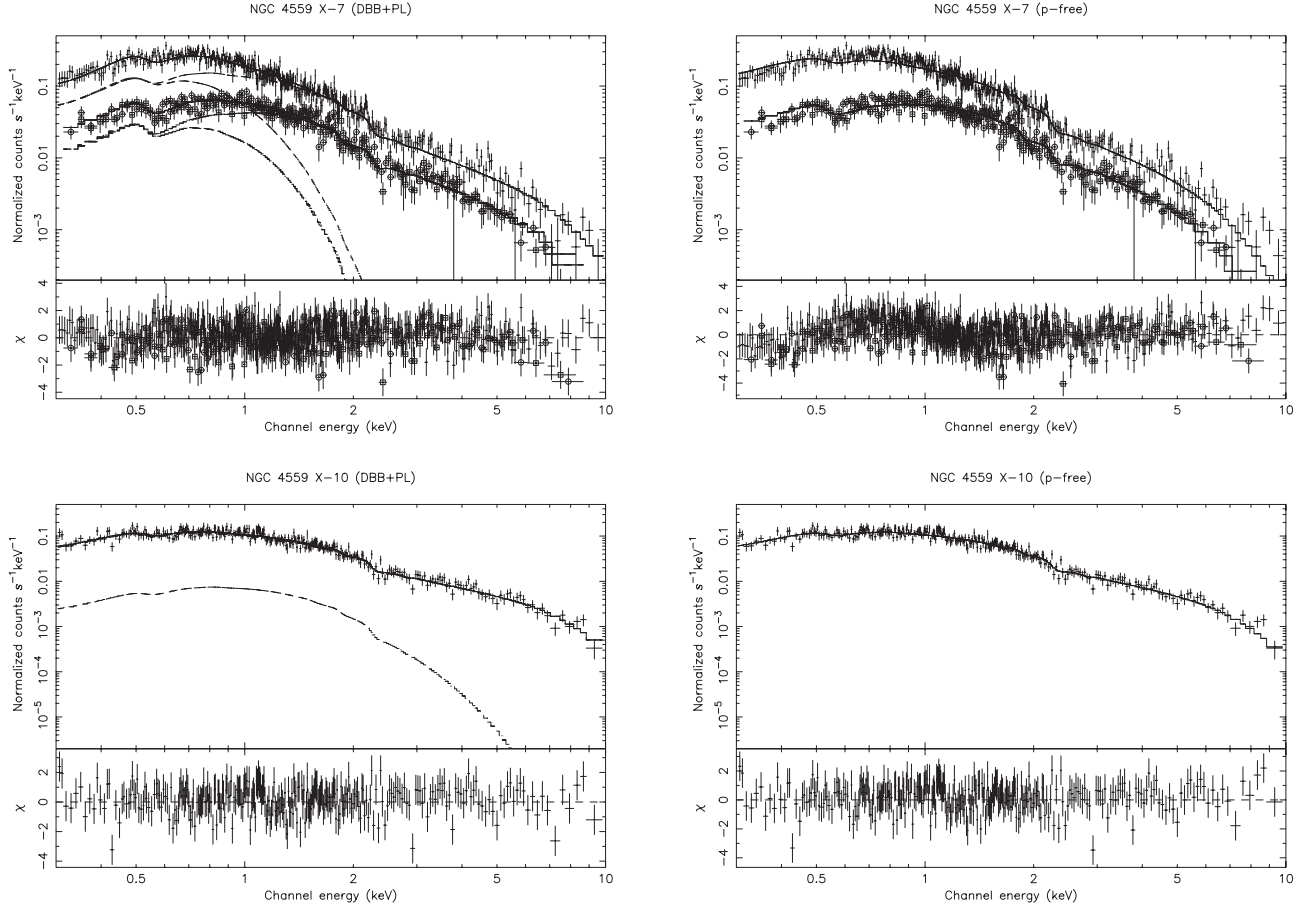


Fig. 1. (Continued.)

**Table 2.** Derived black hole mass value from DBB + PL model and  $p$ -free model in  $M_{\odot}$  and the ratio between the luminosity at 0.3–10 keV and the Eddington luminosity.\*

	NGC 5204 X-1	NGC 4559 X-7	NGC 4559 X-10	NGC 1313 X-2
<b>DBB + PL</b>				
$M(\cos i)^{1/2}$	287	889	118	136
$L(\cos i)^{1/2}/L_E$	0.05	0.03	0.3	0.03
<b><math>p</math>-free</b>				
$M(\cos i)^{1/2}$	$12.5(\kappa/3)^2$	$34.6(\kappa/3)^2$	$12.5(\kappa/3)^2$	$11.2(\kappa/3)^2$
$L(\cos i)^{1/2}/L_E$	$1.1(\kappa/3)^{-2}$	$0.9(\kappa/3)^{-2}$	$2.8(\kappa/3)^{-2}$	$0.4(\kappa/3)^{-2}$

\* We assumed  $\beta \sim 1$  for the DBB + PL model and  $\beta \sim 2/3$  for the  $p$ -free model (see text). The spectral hardening factor,  $\kappa$ , is assumed to be 1.7 for the DBB model, and considered to be  $\approx 3$  for a slim disk.

$$R_{\text{in}} = 3\beta R_s = 8.86\beta \left( \frac{M}{M_{\odot}} \right) \text{ km}, \quad (4)$$

where  $R_s$  is the Schwarzschild radius ( $= 2GM/c^2$ ), by which we can determine the black hole mass. Note that  $1/6 \leq \beta \leq 1$ ,  $\beta = 1/6$  for an extremely rotating Kerr black hole and  $\beta = 1$  for a Schwarzschild black hole.

Here, we used 0.3–10 keV flux,  $f_{[0.3-10\text{keV}]}$ , from which we derived 0.3–10 keV luminosity,  $L_{[0.3-10\text{keV}]}$ . We assumed  $L_{\text{bol}} \approx L_{[0.3-10\text{keV}]}$  because all significant energy range from 0.3 to 10 keV. Therefore, using  $T_{\text{in}}$  and  $f_{[0.3-10\text{keV}]}$  from the fitting

results, we could determine the value of  $R_{\text{in}}$ , black hole mass, and also  $L_{[0.3-10\text{keV}]} / L_E$ , where  $L_E$  is the Eddington luminosity ( $= 1.5 \times 10^{38} M / M_{\odot} \text{ erg s}^{-1}$ ).

### 3.2.2. Problem of DBB + PL model fitting

By using the above equations and the values of  $T_{\text{in}}$  and  $f_{[0.3-10\text{keV}]}$  from the fitting results, we obtained, for the case of NGC 5204 X-1,  $R_{\text{in}} = 2.54 \times 10^3 (\cos i)^{-1/2}$  km and the derived black hole mass of  $287\beta^{-1} (\cos i)^{-1/2} M_{\odot}$ . We also obtained  $L_{[0.3-10\text{keV}]} / L_E = 0.05\beta (\cos i)^{-1/2}$ . In the same way, we obtained a relatively large  $R_{\text{in}}$ , and hence a large black hole mass exceeding  $100 M_{\odot}$  for other sources (see table 2).

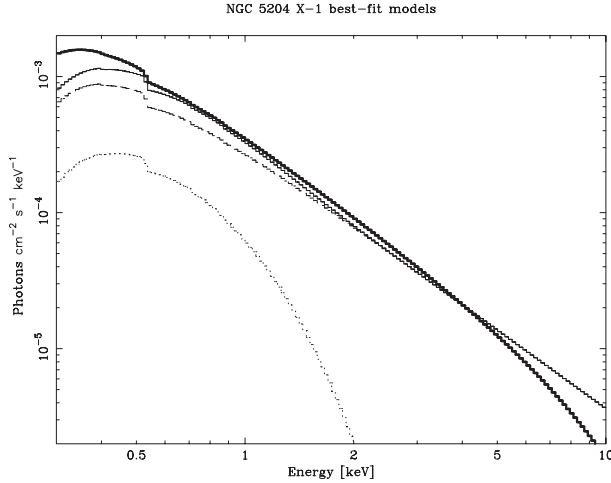


**Fig. 2.** Spectral decompositions of the fits for NGC 5204 X-1. The thinner lines represent, from bottom to top, the disk component, power-law component, and total component, while the thicker line represents the  $p$ -free model.

To summarize, we found through a fitting with the DBB + PL model that the derived black hole masses by far exceed  $100 M_{\odot}$  and are, hence, within the IMBH regime. Thus, fitting the data with the conventional model supports the idea of sub-critical accretion onto the IMBHs.

However, we here point out a serious problem in this interpretation. That is, the spectral decomposition shows that the power-law component predominates in the whole energy region in question (see figure 2 for the case of NGC 5204 X-1). In other words, the disk component only gives a minor contribution to the entire energy ranges for all sources. Therefore, one is never allowed to use equations (1)–(4), which were derived on the assumption that the radiation is for 100% from the DBB component. The black hole mass values derived above cannot be very reliable.

### 3.3. $p$ -Free Model

Next, we tried to fit the same data set by the simplified super-critical disk model alone, i.e., the  $p$ -free disk model.

#### 3.3.1. Fitting results

Firstly, we tried the case of NGC 5204 X-1. Surprisingly we also obtained a good fit with this model, although only a single component was considered (see figure 1). The reduced chi-squared is 1.12. More importantly, we obtained  $p = 0.50 \pm 0.03$ , which is just the value predicted by the theory of a super-critical accretion disk (slim disk: Wang, Zhou 1999; Watarai, Fukue 1999). We also obtained a high-inner disk temperature,  $kT_{\text{in}} = 2.54 \pm 0.34$ , as expected from the large spectral hardening factors, which the slim-disk model predicts.

NGC 5204 X-1 is not an exception (see table 1). We also found a good fit with the  $p$ -free model for the cases of NGC 4559 X-7 and X-10. The  $p$  values of  $0.50 \pm 0.03$  (X-7) and  $0.51 \pm 0.06$  (X-10) and the inner disk temperatures of  $1.84 \pm 0.16$  keV (X-7) and  $3.16 \pm 0.71$  keV (X-10) are again consistent with the slim-disk model.

As for the cases of NGC 1313 X-2, fitting with only the  $p$ -free model also gave a good fit. We obtained,  $kT_{\text{in}} = 2.00 \pm 0.34$  keV, and the  $p$ -value is  $0.50 \pm 0.05$ .

#### 3.3.2. Interpretation of $p$ -free model

It is clear from the results of the fitting with  $p$ -free model that the obtained  $p$  value is around 0.5, indicating super-critical accretion flow (slim disk) for all of the data. Applying a similar interpretation as in the case of fitting with DBB + PL, we obtained,  $R_{\text{in}} = 23.7(\cos i)^{-1/2} (\kappa/1.7)^2$  km, the derived black hole mass of  $2.67\beta^{-1} (\cos i)^{-1/2} (\kappa/1.7)^2 M_{\odot}$  and  $L_{[0.3-10\text{keV}]} / L_{\text{E}} = 5.29\beta (\cos i)^{-1/2} (\kappa/1.7)^{-2}$  for NGC 5204 X-1.

Caution is needed here, however, regarding the inner edge of the disks in the slim disk regimes and the plausible spectral hardening factor values ( $\kappa$ ). Through careful numerical integration, Watarai et al. (2000) found that the inner edge of the disk is substantially smaller,  $R_{\text{in}} \sim R_{\text{S}}$  (i.e.,  $\beta \sim 1/3$ ), in the slim-disk regime, compared with that in the sub-critical (standard disk) regime,  $R_{\text{in}} \sim 3R_{\text{S}}$  ( $\beta \sim 1$ ), even though the central black hole is not rotating. This is because enhanced mass accretion flow with high density finally fills up an empty zone inside  $3R_{\text{S}}$ , which exists in the sub-critical accretion regimes. We then expect significant blackbody emission from inside  $3R_{\text{S}}$ . It is thus preferable to set  $\beta \sim 1/3$ , instead of  $\beta = 1$ . However, radiation from the vicinity of black holes should be attenuated because of intense gravitational redshifts and the transverse Doppler effect, and since the effective temperature corrected for the relativistic effect has a peak at around  $2R_{\text{S}}$ ,  $\beta \sim 2/3$  would be a more reasonable estimate (Kawaguchi 2003).

As for the spectral hardening factor, Shimura and Takahara (1995) and Zampieri et al. (2001) found  $\kappa \approx 1.7$  for stellar-mass black holes, and it increases with increasing  $\dot{M}$ . In a slim disk, the disk temperature becomes higher and the density becomes smaller as  $\dot{M}$  increases; therefore, the electron scattering becomes more dominant and the spectral hardening factor becomes much higher than  $\sim 1.7$  (Kawaguchi 2003). Watarai and Mineshige (2003) found from a comparison between the limit-cycle instability theory (Honma et al. 1991) and the observation of GRS 1915+105 that the spectral hardening factor close to the Eddington luminosity should be about 3.

Because mass estimated from the  $p$ -free models is proportional to  $\kappa^2$ , if we take a larger  $\kappa$ , say, 3, the inferred mass will be tripled compared to the case of standard disks ( $\kappa \sim 1.7$ ). Consequently, adopting  $\beta \sim 2/3$ , our mass estimate is  $12.5(\cos i)^{-1/2} (\kappa/3.0)^2 M_{\odot}$  and the Eddington ratio is  $L_{[0.3-10\text{keV}]} / L_{\text{E}} \sim 1.1(\cos i)^{-1/2} (\kappa/3.0)^{-2}$  for NGC 5204 X-1. In the same manner, we find smaller black hole masses and larger Eddington ratios for other sources (see table 2). The derived black hole mass is well within the stellar-mass black hole regime.

#### 3.4. Fitting Results with Kawaguchi's Model

Finally, we present the results of data fitting with the slim-disk model developed by Kawaguchi (2003) (see Foschini et al. 2005 for the case of ULX M 33 X-8). He developed several models, but we chose a model in which the effects of electron scattering and relativistic correction are included. Calculations were made and fittings were tried for several different values of the viscous parameter,  $\alpha$ . We found that  $\alpha = 0.1$  gives the most satisfactory fits, and will show only the results with  $\alpha = 0.1$  in this paper. The source distance was fixed, and the face-on

**Table 3.** Fitting results with the slim-disk model of Kawaguchi (2003).\*

Fit parameter	NGC 5204 X-1	NGC 4559 X-7	NGC 4559 X-10	NGC 1313 X-2
$N_{\text{H}}$	$0.09 \pm 0.03$	$0.45 \pm 0.03$	$0.69 \pm 0.07$	$1.23 \pm 0.07$
$M$	$18_{-2}^{+2}$	$57_{-4}^{+4}$	$24_{-7}^{+9}$	$12_{-1}^{+1}$
$\dot{M}$	$27_{-4}^{+5}$	$18_{-1}^{+2}$	$100_{-40}^{+70}$	$14_{-1}^{+2}$
$f_{\text{x}}$	1.6	0.79	0.91	0.8
$L_{[0.3-10\text{keV}]} / L_{\text{E}}$	0.81	0.52	1.42	0.36
$\chi^2/\text{dof}$	1.18	1.20	0.93	1.17

\*  $N_{\text{H}}$  is an absorption column external to our Galaxy in units of  $10^{21} \text{ atom cm}^{-2}$ . A Galactic absorption column is assumed as in the text.  $M$  is mass in  $M_{\odot}$ .  $\dot{M}$  is mass accretion rate ( $= L_{\text{Edd}}/c^2$ ).  $f_{\text{x}}$  is the observed flux in units of  $10^{-12} \text{ erg cm}^{-2} \text{ s}^{-1}$  (0.3–10 keV) that depends on the model.

geometry assumed. The model parameters were only the mass and mass-accretion rate (in units of  $L_{\text{Edd}}/c^2$ ). We summarize the fitting results using this model in table 3.

The best fit for NGC 5204 X-1 was obtained with a reduced chi-square value of 1.18, black hole mass of  $18 M_{\odot}$  and a mass-accretion rate of  $27 \dot{M}_{\text{Edd}}$ , where  $\dot{M}_{\text{Edd}} \equiv L_{\text{Edd}}/c^2$ .<sup>1</sup> All of the analyzed data of ULXs could be fitted with Kawaguchi's model, and the derived black hole masses are less than  $100 M_{\odot}$  (see table 3). This is not so surprising for the data showing the slim-disk signatures, because the basic spectral shapes of his model are similar to those of the  $p$ -free model with  $p \sim 0.5$  (as long as  $\dot{M} \gg L_{\text{E}}/c^2$ ).

## 4. Discussion

### 4.1. Accretion Disk Models and Black Hole Mass

In the present study, we re-examined the XMM-Newton data of ULXs through the conventional and more sophisticated spectral models, constructed based on theoretical studies of super-critical accretion flow. We would first like to comment on the results from fitting with DBB + PL and the  $p$ -free model. It is obvious from the fitting results in other papers, e.g. Roberts et al. (2005), Cropper et al. (2004), Miller et al. (2003, 2004), that the DBB + PL model provides a good fit to several ULXs data, and the 'cool' disk temperature obtained from the fitting suggests the existence of IMBHs inside the ULXs. However, we should note that this is only one option, and we tried another option, namely, the  $p$ -free model. Remarkably, the  $p$ -free model also gives a good fit to the same data. Moreover, the obtained  $p$  values, which are  $\sim 0.5$ , indicating the super-critical accretion (slim disk) model, instead of the standard disk (DBB) model, where  $p = 0.75$ . The derived black hole masses and the Eddington ratios also support this conclusion.

Why can the two distinct models give similarly good fits to the data? A trick lies in the spectral slope of the slim-disk model. For a power-law temperature profile,  $T \propto r^{-p}$ , the entire disk spectra, which is the summation of the blackbody emission spectra from various radii, give a power-law spectral slope in the intermediate energy range (below  $h\nu < kT_{\text{in}}$ ) with a spectral slope of  $F_{\nu} \propto \nu^{3-(2/p)}$  (see, e.g., chapter 3 of Kato et al. 1998). Then, the photon index is  $\Gamma = (2/p) - 2$ . That

is, for a slim disk with  $p = 1/2$ , we have  $\Gamma = 2$ . (Note that for a standard disk with  $p = 3/4$  we get  $\Gamma = 2/3$ .) This is a striking coincidence that both the PL model with  $\Gamma = 2$  and the slim disk model give the same power-law spectra in the moderate energy range. To see this more explicitly, we show in figure 2 the two fitting models with fitting parameters obtained for NGC 5204 X-1. We see that both the DBB + PL model and the slim-disk model produce a power-law decline with a power-law index of  $\sim -1$  (or photon index,  $\Gamma \sim 2$ ), and are identical at the 0.5–5 keV energy range.

In the present work, it was hardly possible from model fitting to judge if the DBB + power-law model or the slim-disk model is preferable, being limited by photon statistics. It is, however, in principle possible to distinguish the two models by measuring their spectra very accurately. So far, XMM-Newton has been able to do this only for M 82 X-1, the brightest ULX (Okajima et al. 2006). Okajima et al. (2006) found that the energy spectrum of M 82 X-1 above  $\sim 3$  keV has a curvature just between the power-law and DBB model, and is represented pretty well with a  $p$ -free model of  $p = 0.61$ . This is considered to be strong evidence of slim disks in ULXs. The next-generation hard X-ray satellites with higher sensitivity and imaging capability are expected to precisely measure the energy spectra of most ULXs, so that the black hole parameters are constrained by applying precise slim-disk model spectra.

### 4.2. Luminosity–Temperature Diagram

Then, which is more likely to be the case, sub-critical accretion onto intermediate-mass black holes or super-critical accretion onto stellar-mass black holes?

We pointed out a serious problem inherited from the DBB + PL model. The spectral fitting with the DBB + PL model shows that the power-law component predominates in all energy regions (figure 2). In other words, the disk contribution is very small compared to the power-law contribution, and therefore the black hole masses derived above might not be very reliable, because the standard disk relations cannot be used here.

On the other hand, a good fit with the  $p$ -free model alone implies that the disk contributes in all energy regions; therefore, the black hole masses derived from the fitting with  $p$ -free model can be reliable. For these reasons, we can safely conclude that the latter model is more likely to explain the physics of ULXs.

<sup>1</sup> Here,  $16L_{\text{Edd}}/c^2$  is the critical accretion rate, which would produce Eddington luminosity in the case of a classical radiative efficiency (1/16).

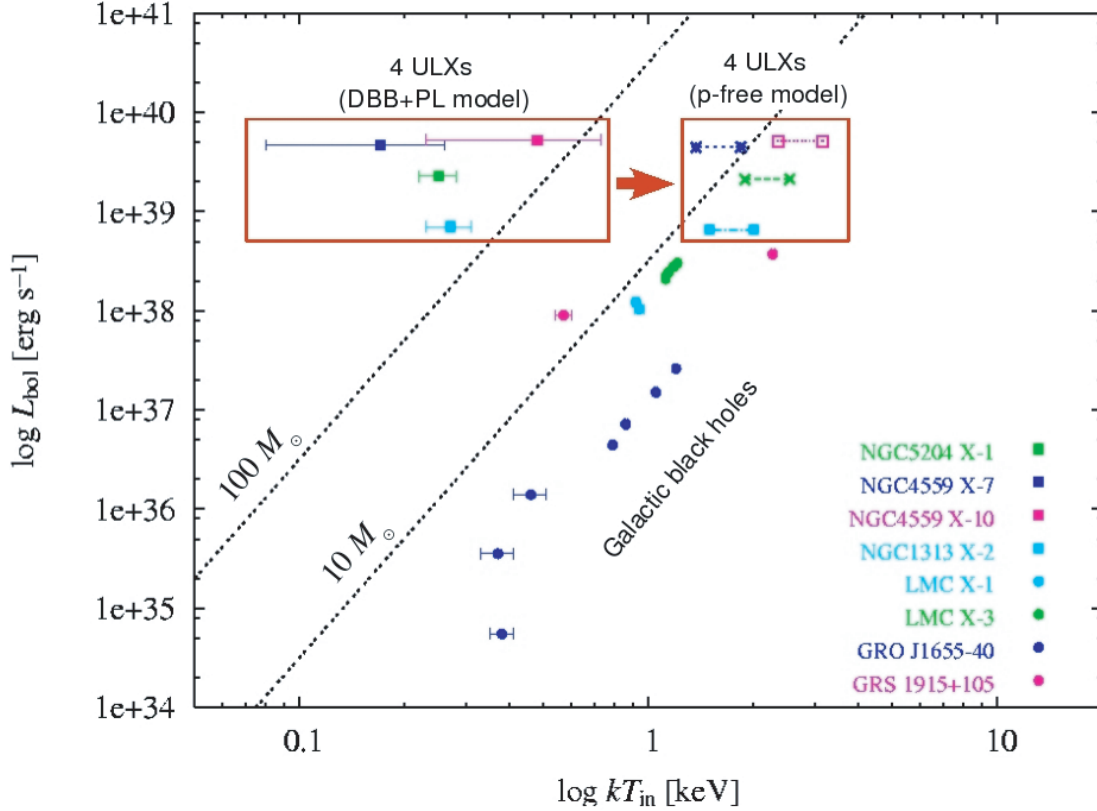


**Fig. 3.** Relation between the luminosity at 0.3–10 keV ( $L_{[0.3-10\text{keV}]}$ ) and  $T_{\text{in}}$  for ULXs and stellar mass black hole candidates (BHCs). BHCs references: Ebisawa (1991 for LMC X-1), Treves et al. (1988 for LMC X-3), Mendez et al. (1998 for GRO J1655–40), and Belloni et al. (1997 for GRS 1915+105). Note that in this figure  $L_{\text{bol}}$  means the 0.3–10 keV luminosity for ULXs and the bolometric luminosity for Galactic black hole candidates, both assuming the face-on geometry. The ranges of  $T_{\text{in}}$  in the  $p$ -free model box represent the values via DBB model (lowest end) and  $p$ -free model (highest end).

We summarize our results in figure 3. This is a temperature-luminosity diagram (cf. Makishima et al. 2000; cf. Miller et al. 2004) with the lines of constant black-hole masses. We plot our ULXs fitting results with DBB+PL and the  $p$ -free models together with several best-studied stellar-mass black hole candidates (BHCs). We can see that the low temperatures obtained from the fitting using the DBB+PL model are shifted to higher temperatures when fitted with the  $p$ -free model. This implies that the black hole mass values in the range of IMBHs obtained from the fitting with the DBB+PL model can be shifted to the stellar-mass range by the  $p$ -free model; that is, still there is so far no evidence of IMBHs, at least in four ULXs investigated in this paper, due to the minor disk contribution in the DBB+PL model, as mentioned before.

It then naturally follows that all of the fitting results that gave low disk temperatures and photon indices of  $\Gamma \sim 2$  should be re-examined, since those data are very likely to be fitted with the slim-disk ( $p$ -free) model equally well. Obviously, the latter model gives higher disk temperatures, and hence lower black hole masses. It is, in this respect, interesting to note the statistical study of ULXs by Winter et al. (2006), who examined the distribution of photon indices, and found a concentration at  $\Gamma \sim 2$  for the high-state ULXs, those ULXs whose spectra can well be fitted with the combined DBB+PL model. Some of them may be in the slim-disk regimes, rather than in the high state.

## 5. Conclusion

We have investigated the XMM-Newton EPIC spectra of the four ULXs which were claimed to be strong candidates of IMBHs by several authors. We found that these spectra could be successfully fitted with slim-disk models, and the derived masses are  $\sim 11$  to  $60 M_{\odot}$ , depending on the different assumptions. We have not seen any evidence of “intermediate mass” black holes having several hundreds of  $M_{\odot}$ . When the mass-accretion rate is close to, or exceeding, the critical rates, a slim disk is theoretically predicted. We suggest that ULXs are stellar-mass black holes, at most several tens of  $M_{\odot}$  under super-critical accretion rates shining at super-Eddington luminosities.

We gratefully thank Marek Abramowicz for valuable comments and suggestions. This work was supported in part by Grants-in-Aid of the Ministry of Education, Science, Culture, and Sport (14079205, 16340057 S.M.), by the Grant-in-Aid for the 21st Century COE “Center for Diversity and Universality in Physics” from the Ministry of Education, Culture, Sports, Science and Technology (MEXT). K.V. gratefully thank Ken-ya Watarai for the discussions at some beginnings of this work and also MEXT scholarship. T.K. gives thanks for financial support from JSPS Postdoctoral Fellowship (01879).



## References

- Abramowicz, M. A., Calvani, M., & Nobili, L. 1980, *ApJ*, 242, 772
- Abramowicz, M. A., Czerny, B., Lasota, J. P., & Szuszkiewicz, E. 1988, *ApJ*, 332, 646
- Abramowicz, M., Jaroszyński, M., & Sikora, M. 1978, *A&A*, 63, 221
- Abramowicz, M. A., Kato, S., & Matsumoto, R. 1989, *PASJ*, 41, 1215
- Abramowicz, M. A., Kluźniak, W., McClintock, J. E., & Remillard, R. A. 2004, *ApJ*, 609, L63
- Belloni, T., Méndez, M., King, A. R., van der Klis, M., & van Paradijs, J. 1997, *ApJ*, 479, L145
- Colbert, E. J. M., Petre, R., Schlegel, E. M., & Ryder, S. D. 1995, *ApJ*, 446, 177
- Colbert, E. J. M., & Ptak, A. F. 2002, *ApJS*, 143, 25
- Cropper, M., Soria, R., Mushotzky, R. F., Wu, K., Markwardt, C. B., & Pakull, M. 2004, *MNRAS*, 349, 39
- Davis, S. W., Done, C., & Blaes, O. M. 2006, *ApJ*, 647, 525
- Dickey, J. M., & Lockman, F. J. 1990, *ARA&A*, 28, 215
- Ebisawa, K., Makino, F., Mitsuda, K., Belloni, T., Cowley, A. P., Schmidtke, P. C., & Treves, A. 1993, *ApJ*, 403, 684
- Ebisawa, K., Mitsuda, K., & Hanawa, T. 1991, *ApJ*, 367, 213
- Ebisawa, K., Życki, P., Kubota, A., Mizuno, T., & Watarai, K. 2003, *ApJ*, 597, 780
- Fabbiano, G. 1989, *ARA&A*, 27, 87
- Foschini, L., et al. 2005, *astro-ph/0506298*
- Gierliński, M., Maciolek-Niedźwiecki, A., & Ebisawa, K. 2001, *MNRAS*, 325, 1253
- Honma, F., Kato, S., & Matsumoto, R. 1991, *PASJ*, 43, 147
- Kato, S., Fukue, J., & Mineshige, S. 1998, *Black-Hole Accretion Disks* (Kyoto: Kyoto University Press)
- Kawaguchi, T. 2003, *ApJ*, 593, 69
- King, A. R. 2004, *MNRAS*, 347, L18
- King, A. R., Davies, M. B., Ward, M. J., Fabbiano, G., & Elvis, M. 2001, *ApJ*, 552, L109
- Körding, E., Falcke, H., & Markoff, S. 2002, *A&A*, 382, L13
- Lachowicz, P., Czerny, B., & Abramowicz, M. A. 2006, *astro-ph/0607594*
- Madhusudhan, N., Justham, S., Nelson, L., Paxton, B., Pfahl, E., Podsiadlowski, Ph., & Rappaport, S. 2006, *ApJ*, 640, 918
- Makishima, K., et al. 2000, *ApJ*, 535, 632
- McClintock, J. E., & Remillard, R. A. 2006, in *Compact Stellar X-ray Sources*, ed. W. H. G. Lewin & H. van der Klis (Cambridge UK: Cambridge University Press), 157
- McClintock, J. E., Shafee, R., Narayan, R., Remillard, R. A., Davis, S. W., & Li, L.-X. 2006, *ApJ* in press, *astro-ph/0606076*
- Méndez, M., Belloni, T., & van der Klis, M. 1998, *ApJ*, 499, L187
- Miller, J. M., Fabbiano, G., Miller, M. C., & Fabian, A. C. 2003, *ApJ*, 585, L37
- Miller, J. M., Fabian, A. C., & Miller, M. C. 2004, *ApJ*, 614, L117
- Mineshige, S., Hirano, A., Kitamoto, S., Yamada, T. T., & Fukue, J. 1994, *ApJ*, 426, 308
- Mucciarelli, P., Casella, P., Belloni, T., Zampieri, L., & Ranalli, P. 2006, *MNRAS*, 365, 1123
- Okajima, T., Ebisawa, K., & Kawaguchi, T. 2006, *ApJL* submitted
- Pakull, M. W., & Mirioni, L. 2002, in *Proc. New Visions of the X-ray Universe in the XMM-Newton and Chandra Era*, *astro-ph/0202488*
- Ptak, A., & Colbert, E. 2004, *ApJ*, 606, 291
- Reynolds, C. S., Loan, A. J., Fabian, A. C., Makishima, K., Brandt, W. N., & Mizuno, T. 1997, *MNRAS*, 286, 349
- Roberts, T. P., & Warwick, R. S. 2000, *MNRAS*, 315, 98
- Roberts, T. P., Warwick, R. S., Ward, M. J., Goad, M. R., & Jenkins, L. P. 2005, *MNRAS*, 357, 1363
- Shafee, R., McClintock, J. E., Narayan, R., Davis, S. W., Li, L.-X., & Remillard, R. A. 2006, *ApJ*, 636, L113
- Shimura, T., & Takahara, F. 1995, *ApJ*, 445, 780
- Strohmer, T. E., & Mushotzky, R. F. 2003, *ApJ*, 586, L61
- Török, G. 2005, *A&A*, 440, 1
- Treves, A., Belloni, T., Chiappetti, L., Maraschi, L., Stella, L., Tanzi, E. G., & van der Klis, M. 1988, *ApJ*, 325, 119
- Wang, D. Q. 2002, *MNRAS*, 332, 764
- Wang, J.-M., & Zhou, Y.-Y. 1999, *ApJ*, 516, 420
- Watarai, K., & Fukue, J. 1999, *PASJ*, 51, 725
- Watarai, K., Fukue, J., Takeuchi, M., & Mineshige, S. 2000, *PASJ*, 52, 133
- Watarai, K., & Mineshige, S. 2003, *ApJ*, 596, 421
- Watarai, K., Mizuno, T., & Mineshige, S. 2001, *ApJ*, 549, L77
- Winter, L. M., Mushotzky, R. F., & Reynolds, C. S. 2006, *ApJ*, 649, 730
- Zampieri, L., Turolla, R., & Szuszkiewicz, E. 2001, *MNRAS*, 325, 1266